Formation of discontinuous tracks in single-crystalline InP by 250-MeV Xe-ion irradiation

O. Herre, W. Wesch,* and E. Wendler
Friedrich-Schiller-Universität Jena, Institut für Festkörperphysik, Max-Wien-Platz 1, D-07743 Jena, Germany

P. I. Gaiduk and F. F. Komarov
State University of Belarus, Institute of Applied Physics Problems, Kurchatova 7, 220062 Minsk, Belarus

S. Klaumünzer and P. Meier
Hahn-Meitner-Institut Berlin, Glienicker Strasse 100, D-14109 Berlin, Germany
(Received 27 January 1998)

Damage production was studied in 250-MeV Xe-ion irradiated single-crystalline InP by means of Rutherford backscattering spectrometry using a channeling technique and cross-section TEM. Different concentrations and types of defects are created at different depths of the trajectory due to the different dominating interaction processes. Depending on the ion fluence the formation of discontinuous tracks and amorphous layers was registered in the depth region of high electronic energy loss of the incident ions. The observed findings are interpreted as the effect of a thermal spike in combination with damage accumulation resulting from imperfect epitaxial recrystallization of the molten ion tracks. [S0163-1829(98)05432-0]

I. INTRODUCTION

Latent track formation is well known in insulating materials as well as in some intermetallic compounds and pure metals due to the high electronic excitation energy density produced by inelastic collisions between the fast projectile ions and the target electrons (see Refs. 1–3 and references therein). The physical situation is less clear with semiconductors. In amorphous Si and Ge crystalline tracks were found.[4] Track formation has also been reported in high-resistivity crystalline semiconductors,[1] and elliptical latent tracks with amorphous cores were recently registered by high-resolution transmission electron microscopy in single-crystalline GeS implanted with heavy ions at energies of 5.9–13 MeV/u.[5] In wide-gap semiconductors (such as diamond and BN_3) high-pressure local regions were observed to correlate well with the depth distribution of the electronic stopping power and were interpreted as to be due to tracks.[6,7] In conventional and technologically important crystalline semiconductors no indication of track formation has been reported until now. It has been shown that high electronic energy deposition seems to be inefficient for the production of damage in Si (Ref. 8) and 6H-SiC.[9] Rather, what is experimentally found for several semiconductors such as Si, Ge, GaAs, and GaP (Refs. 8 and 10–13) is that during high-energy ion irradiation an *in situ* damage annealing occurs that is obviously correlated with the high electronic energy deposition. In the case of irradiation of amorphized InP it has been found[14] that for irradiation with 30-MeV Se ions at low temperatures the electronic energy loss causes a lateral shift of the bombarded surface area and this effect has been ascribed to the generation of a molten zone around the ion trajectory.[14,15] To study the effect of the electronic energy loss on damage formation in more detail we have investigated the damage in InP due to 250-MeV Xe-ion irradiation at room temperature by means of the Rutherford backscattering spectrometry using a channeling technique (RBSC) and cross-section transmission electron microscopy (TEM).

II. EXPERIMENT

⟨100⟩ InP was irradiated with 250-MeV Xe ions at room temperature. The ion fluence N_I was varied between 5×10^{12} and 1×10^{14} Xe cm^{-2}. Uniform irradiation was performed by beam scanning. To prevent sample heating during the high-energy irradiation the flux was kept constant below 1.3×10^{10} Xe cm^{-2} s^{-1} and the ⟨100⟩ InP samples were mounted to the sample holder with a silver paste giving a good thermal conductivity between them.

The implanted layers were investigated by means of the RBSC and TEM in combination with cross-section preparation. The RBS measurements were carried out using 1.4-MeV He^+ ions and a backscattering angle of $\theta=170°$. Under these conditions the depth, which can be clearly analyzed in a quantitative manner in InP, is approximately 0.6 μm, i.e., one obtains information about a depth region in which the interaction of the implanted Xe ions with the InP crystal is determined by electronic stopping. Assuming a random distribution of the atoms displaced by the Xe ions within the lattice cell, from the measured RBS spectra the depth distribution of the relative concentration of displaced lattice atoms n_{da} was calculated in the framework of the discontinuous model of the dechanneling.[16] The TEM investigations were carried out with an electron microscope EM-125 operating at 100 keV. By means of an ion beam sputtering equipment both plane-view and cross-section preparations were carried out. In order to prevent sample heating and artifacts of etching (e.g., selective sputtering and In segregation on the surface) ion beam milling was performed at low temperatures and the angle between the milling ion beam and the sample surface was lower than 7°.

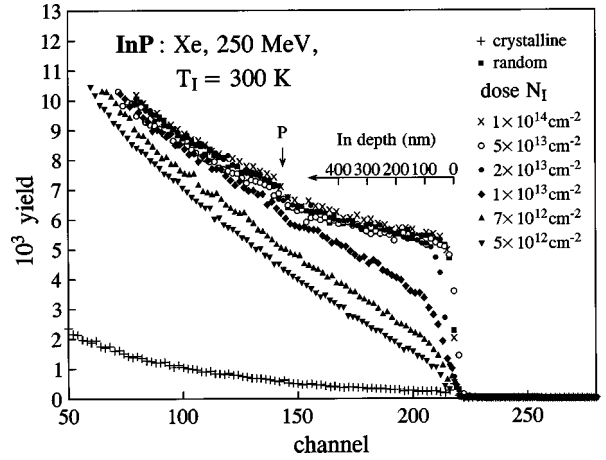

FIG. 1. Energy spectra of 1.4-MeV He ions backscattered on 250-MeV Xe-implanted InP for various ion fluences.

III. RESULTS AND DISCUSSION

The RBS spectra of the implanted InP samples are represented in Fig. 1. The yield of He^+ ions backscattered in the near surface region increases with increasing ion dose and reaches the random level for fluences $N_I > 2 \times 10^{13}$ Xe cm^{-2}, which is commonly an indication for the formation of an amorphous layer. It should be mentioned that already at $N_I = 5 \times 10^{12}$ Xe cm^{-2} the backscattering yield is remarkably increased with respect to that of the virgin crystal due to defects within the irradiated layer. Figure 2 shows the concentration of displaced atoms n_{da} for the various ion fluences as a function of the depth z, which were calculated from the RBS spectra depicted in Fig. 1. It can be seen that in the depth region above ≈ 0.1 μm n_{da} remains nearly constant and increases with the ion fluence until the maximum value $n_{da} = 1$ is reached for ion fluences $N_I \geqslant 2.5 \times 10^{13}$ cm^{-2} indicating the formation of an amorphous layer. It should be mentioned that the damage detected by RBS is small immediately below the surface. Similar values of n_{da} are obtained when the irradiation temperature is reduced to liquid-nitrogen temperature. Furthermore, the storage of the samples at room temperature for a period of 1 yr and repetition of the RBS measurements reproduces the original values. We conclude from these findings that a long-term thermally activated migration of defects does not play a significant role for the processes described in this paper.

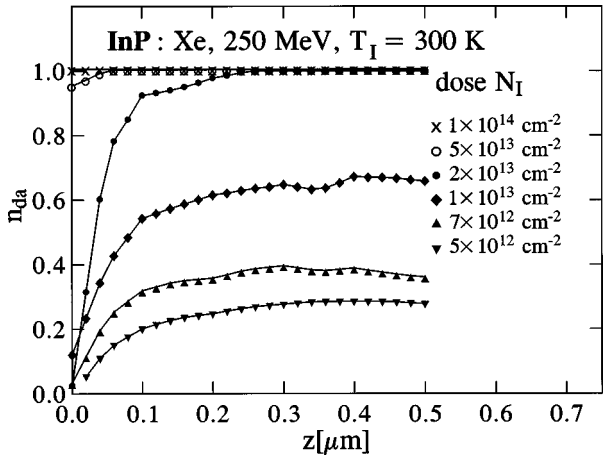

FIG. 2. Concentration of displaced atoms n_{da} calculated from the energy spectra in Fig. 1 as a function of depth z.

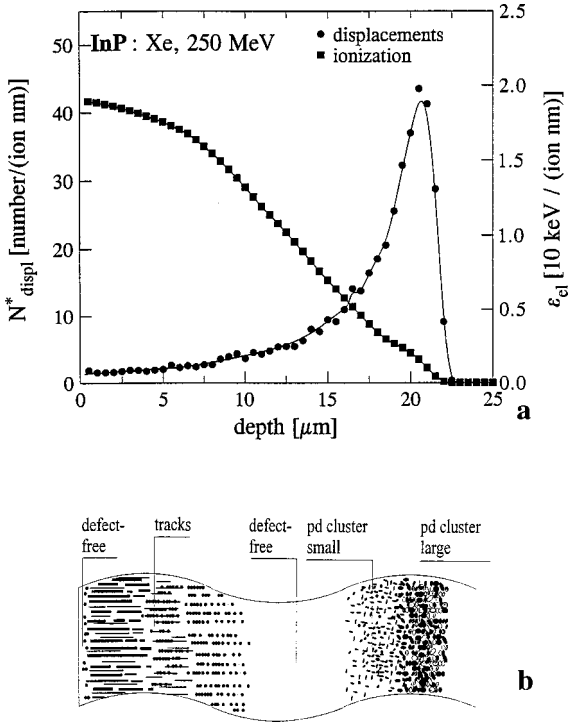

FIG. 3. (a) Calculated (TRIM 87) number of primary displacements N^*_{displ} and electronic energy loss $\varepsilon_{\mathrm{el}}$ per ion and unit depth versus the depth for 250-MeV Xe-ion irradiation and (b) schematic illustration of the damage structure over the whole implanted depth as deduced from TEM investigations.

For a better understanding of the results given in Fig. 2 the energy deposition mechanisms occurring during ion irradiation have to be considered. Figure 3(a) shows the depth distribution of the electronic energy loss $\varepsilon_{\mathrm{el}}$ (ionization) and of the number of displacements (representing the nuclear energy deposition) N^*_{displ} per incident Xe ion and unit depth, which were calculated by the TRIM95 code[17] using a displacement threshold of 8 eV. It is clearly to be seen that in the depth region down to ≈ 8 μm the electronic energy deposition dominates. It therefore can be supposed that the damage produced by the 250-MeV Xe ions in the near surface region (see Fig. 2) may be mainly connected with ionization processes.

In order to compare these results with that obtained for conventional ion energies (several 100 keV to a few MeV; see, e.g., Refs. 13, 18, and 19), the ion fluence is recalculated into displacements per lattice atom $\mathcal{D}$ according to $\mathcal{D} = N^*_{\mathrm{displ}} N_I / N_0$ (N_0 is the atomic density of the target). Using $N^*_{\mathrm{displ}} = 1.6/(\text{ion nm})$ in the depth region up to 1 μm [Fig. 3(a)], the ion fluence $N_I = 7 \times 10^{12}$ Xe cm^{-2}, which leads to a relative concentration $n_{da} \approx 0.37$ of displaced atoms (see Fig. 2), corresponds to 3×10^{-3} $\mathcal{D}$. For this number of displacements per atom in the case of conventional ion energies a defect concentration $n_{da} \ll 0.05$ results (see Ref. 13), which is much smaller than the value found for the 250-MeV Xe irradiation. The ion fluence 1×10^{14} Xe cm^{-2} which, according to the RBS analysis, results in the formation of an amorphous layer, corresponds to 0.041 $\mathcal{D}$. It has been previously

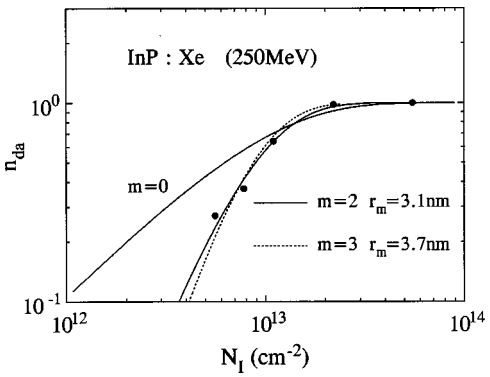

FIG. 4. Concentration n_{da} of displaced atoms determined from the RBS spectra and curves calculated according to the overlap damage model for various overlap numbers versus the ion dose N_I.

shown that, depending on the ion mass, a nuclear energy deposition corresponding to 0.2 $\mathcal{D}$ [300 and 600-keV Se (Ref. 13)] to 1 $\mathcal{D}$ [100-keV B (Ref. 19)] is necessary to amorphize InP. These results allow the conclusion that the damage observed after 250-MeV Xe irradiation by RBS is not due to the nuclear but the high electronic energy deposition.

If the damaged regions remaining after the energy dissipation has finished are stable, which can be assumed for InP at room temperature, the damage evolution can be described in the framework of the overlap damage model introduced by Gibbons.[20] In this model it is assumed that amorphous regions are produced if m ions impinge within the same area of the crystal. According to this model, the ratio between the total surface area A_A covered by amorphous clusters and the total area A_0 being implanted is given by

$$\frac{A_A}{A_0}=1-e^{-A_I N_I}\sum_{k=0}^{m}\frac{(A_I N_I)^k}{k!},$$

with $A_I=\pi r_m^2$ being the surface area damaged by a single ion and m being the overlap number ($m=0$ corresponds to direct amorphization by the first impinging ion). We use this model to describe the dose dependence of n_{da}. However, it should be mentioned that the quantity n_{da} determined from RBS measurements gives the total concentration of displaced lattice atoms, i.e., contains information not only about amorphous regions but also about point defects and point-defect complexes. This means that the use of this quantity overestimates the amorphous fraction. In Fig. 4 the concentration n_{da} of displaced atoms determined from the RBS spectra (see Fig. 2) as well as curves calculated according to the overlap damage model for overlap numbers $m=0,2,3$ are depicted versus the ion fluence. The best agreement with the experimental data is obtained for $m=2$ or 3, i.e., three or four ions must impinge the same area to produce amorphous material. It is important to note that direct amorphization ($m=0$) does not give a satisfactory description of the experimental data (see Fig. 4). This is in contrast to results obtained for fast heavy ion irradiation into high-T_c superconductors where each impinging ion produces a track.[21] Our RBS results on InP indicate that in this material the formation of amorphous regions due to electronic excitation requires predamaging.

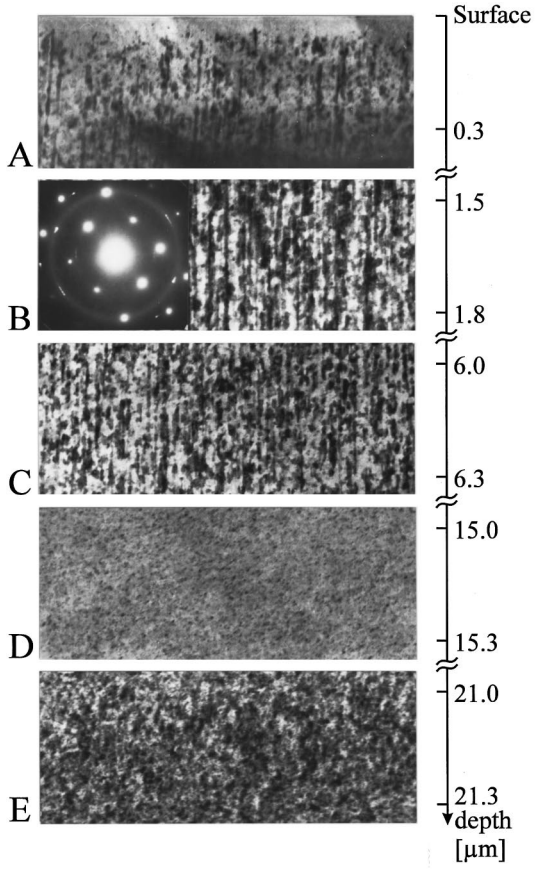

FIG. 5. Bright-field XTEM images of 250-MeV Xe-implanted InP for $N_I=7\times10^{12}$ cm^{-2} obtained at different depths. In *B* also the corresponding diffraction pattern is given.

More detailed information on the morphology and the kind of defects in the implanted layers is obtained from the TEM investigations. Figure 5 shows bright-field cross-section TEM (XTEM) images of the sample implanted with $N_I=7\times10^{12}$ Xe cm^{-2} at various depths.

A thin surface layer of about 35 nm thickness is just slightly damaged. At depths between about 15 and 35 nm a few black spots are visible with size of about 2–3 nm (part A of Fig. 5). The analysis of the contrast in different diffraction conditions allows the conclusion that these black spots are presumably clusters of point defects and probably small-sized amorphous inclusions. It should be mentioned that ion implantation using conventional ion energies yields also a thin crystalline InP layer at the surface.[19] Therefore, it can be assumed that the appearance of this surface layer is a surface effect that is independent of the ion energy.

In the depth region 40–100 nm a great number of tracks of isolated spherical or elongated cylindrical defect clusters distributed along the ion trajectory are formed. In addition to these columnar defects a number of clusters of point defects as well as small amorphous inclusions 2–5 nm in size are found to be randomly distributed in the corresponding depth region.

In the depth region between 100 nm, and about 10 μm (parts $A-C$ in Fig. 5) straight lines with a dark contrast can be seen in the bright-field XTEM images. The straight lines include an angle of 86° with respect to the surface corresponding to the angle of incidence of the Xe ions. Plane-

view TEM images (not shown here) revealed a nearly circular shape of the cross section of these damage regions; their diameter and number density were estimated to be about 7–15 nm and $1-(2\times10^{11})$ cm^{-2}, respectively. This means that the number of tracks produced is significantly smaller than the number of impinging ions. The presence of diffuse rings and pronounced spots in the microdiffraction pattern (see the inset in part B of Fig. 5) allows the conclusion that the inner structure of these columnar defects consists of a mixture of amorphous InP and probably a small amount of fine polycrystalline grains. All these features indicate that the columnar defects are tracks produced in InP by the slowing down of 250-MeV Xe ions due to the electronic stopping.

Behind the track region, at depths between 10 and 17 μm, the existence of single-crystalline InP was registered, which contains only clusters of point defects (see part *D* of Fig. 5). Finally, a band of heavily damaged InP (part *E* of Fig. 5) occurs at a depth of about 19–21 μm. The damage structure was identified to consist of a mixture of amorphous and crystalline regions. This depth of damage correlates well with the maximum of nuclear energy deposition as calculated by TRIM 95 [see Fig. 3(a)]. Therefore, it seems to be obvious that the collision cascades due to the nuclear energy loss of the Xe ions are responsible for the damage production in this depth region. A schematic illustration of the damage structure over the whole implanted depth as deduced from the TEM investigations on the sample implanted with 7×10^{12} Xe cm^{-2} is shown in Fig. 3(b).

The existence of the intermediate single-crystalline InP layer supports again the conclusion that the electronic energy deposition and not the small amount of nuclear energy loss is responsible for the defect production in the front depth region because otherwise the intermediate crystalline region where the nuclear energy deposition is still higher than near the surface ($\approx$10 displacements per ion and nm corresponding to 0.017 $\mathcal{D}$) should not exist. Further, it follows that defects are only produced by the electronic energy loss if the latter exceeds a critical value of about 12–13 keV/nm, which is reached at a depth of about 10 μm (see Fig. 3).

In Fig. 6 the results of the TEM investigations of the InP sample irradiated with 5×10^{13} Xe cm^{-2} are shown. Part *A* of Fig. 6 gives an example of cross-section bright-field images and diffraction patterns obtained from the near surface region up to the depth of about 12 μm. It can be seen that this depth region consists of amorphous InP with some crystallites embedded.

Further, the diffraction pattern indicates that the crystallites have the orientation of the substrate (pronounced spots). At depths between 15 and 19 μm single-crystalline InP containing only clusters of point defects (not shown) is observed, similar to that found for $N_I=7\times10^{12}$ Xe cm^{-2} (see part *D* of Fig. 5). Between the amorphous layer and the region of single-crystalline InP a transition region exists in which spherical or elongated cylindrical crystalline zones are distributed along the direction of the trajectory of the ions (see part *B* of Fig. 6). The diffraction pattern of this transition region reveals the existence of amorphous and defective crystalline InP. Behind the intermediate single-crystalline region again, as in the case of 7×10^{12} Xe cm^{-2}, the region of damage production by nuclear energy loss can be seen, which appears to be an amorphous layer extending from 19 to 21 μm (not shown). The ion fluence $N_I=5\times10^{13}$ Xe cm^{-2} corresponds to 0.55 $\mathcal{D}$ in the maximum of the distribution and for this value amorphization of InP is also found for conventional energies.[13,18]

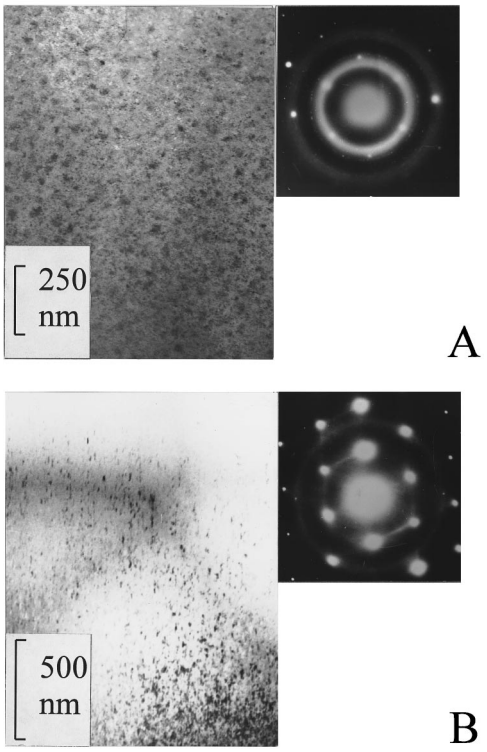

FIG. 6. Bright-field XTEM images and diffraction pattern of 250-MeV Xe-implanted InP for $N_I=5\times10^{13}$ cm^{-2} obtained at different depths.

In summarizing the major experimental results of this work we can say that the concentration and the structure of the damage produced by electronic excitations depend on the ion fluence. At small fluences only point defects and point defect complexes are detected. With increasing ion fluence discontinuous tracks and subsequently amorphous layers are formed. This fluence dependence indicates that a single ion impinging on virgin crystalline InP generates only point defects and point-defect complexes. Amorphous tracks appear only if a critical concentration of these defect centres exists. Such a mechanism of track formation during fast heavy ion irradiation has not been reported until now; for the other materials investigated only an energy[1,2] and velocity dependence are known.[22,23] So from our experimental findings two questions arise. (i) How are the point defects and point-defect complexes produced? (ii) What is the reason for the appearance of amorphous tracks?

An often used description of track formation in solids is based on the thermal spike model. In this model it is assumed that the material melts along the ion trajectory up to depths for which the electronic energy loss exceeds a certain critical value followed by fast cooling and resolidification so that an amorphous track is formed within a crystalline surrounding.[24,25] The critical energy loss depends on the target material and reflects the efficiency of the mechanism, which converts electronic excitation energy into atomic motion, in comparison with concurrent mechanisms, which dissipate the excitation energy into the bulk. From laser experi-

ments it is known that above a certain excitation level the lattice of silicon and GaAs is unstable on a time scale of 100 fs.[26,27] We assume that this 100-fs instability of the diamond lattice works also in InP and provides the mechanism that converts a significant fraction of the energy deposited into electronic excitation by a 250-MeV Xe ion into atomic motion long before diffusion of electrons and holes dissipate the excitation energy in the bulk material. Stampfli and Bennemann[26,27] calculated that excitation of about 10% of the valence electrons into the conduction band is sufficient to induce this lattice instability. The minimum electronic excitation energy density, $\varepsilon_{\min}$ is thus

$$\varepsilon_{\min}=0.1 n_e E_g N_a \approx 2.2\times 10^{22}\ \text{eV cm}^{-3},$$

where $n_e=4$ is the number of valence electrons per atom, $E_g=1.4$ eV is the energy gap of InP, and $N_a=3.92\times 10^{22}$ atoms cm^{-3}. To convert the electronic energy loss ε_{el} into an electronic energy density we take into account that roughly one half of ε_{el} is deposited within a core of radius $r_c=v_p/\omega_p$, where v_p is the projectile velocity and ω_p is the plasma frequency of the target material. The other half of ε_{el} produces high-energy δ rays that leave the core region and, dissipating their energy far away from the core, are considered here as being inefficient for damage production. For the ions of this work r_c is about 4 nm. Therefore, we obtain for $\varepsilon_{\text{el,min}}=13$ keV/nm (see Fig. 3)

$$\varepsilon_{\min}=\tfrac{1}{2}\varepsilon_{\text{el,min}}(\pi r_c^2)^{-1}\approx 1\times 10^{23}\ \text{eV cm}^{-3}.$$

This value is about a factor of 5 larger than the theoretical value having enough room for further concurrent dissipation processes. We conclude that the 100-fs lattice instability may provide a basis for a quantitative understanding.

After the lattice has become unstable subsequent collisions between the moving atoms lead to a rapid melting of the core.[26,27] In a virgin sample this molten core is surrounded by a perfect crystal and, during the quenching of the thermal spike on time scale of 10 ps, epitaxial recrystallization must take place to be in accordance with the experimental findings of this work. Obviously, this recrystallization is not perfect, but many defects and defect clusters remain. An identical behavior was previously found in crystalline GaAs, which contains a high concentration of point defects and point-defect complexes after laser-induced melting.[28] When a second ion impinges the target nearby recrystallization of the molten core may be hindered because the surrounding crystal is now less perfect. With ongoing irradiation the recrystallization speed may become smaller than the cooling rate and a rather continuous amorphous track is frozen in.

Since the quenching of the spike occurs in less than 100 ps,[24] more or less perfect epitaxial recrystallization of the molten core of the first two ions (within the area A_I) implies recrystallization velocities v_c larger than 33 m/s. This value is larger than the maximum v_c of about 20 m/s for a planar liquid-solid interface of silicon at ambient (zero) pressure.[28,29] We expect that a similar maximum v_c exists for InP. However, it should be kept in mind that the molten core has neither a planar liquid-solid interface nor is it under zero pressure. It is presently an open question whether both effects enhance v_c to the magnitude needed to render the proposed multi-impact model self-consistent.

IV. SUMMARY

The formation of amorphous tracks and completely amorphous layers in single-crystalline InP after swift heavy ion irradiation with 250-MeV Xe has been demonstrated in the depth region between 35 nm and about 10 μm. This depth region corresponds to the region where the impinging ions lose their energy preferentially via electronic excitation of the target atoms. One can infer from this depth distribution that the electronic energy loss per ion and unit length has to exceed a critical value of $\varepsilon_{\text{el,min}}\approx 13$ keV/nm to damage single-crystalline InP.

*Author to whom correspondence should be addressed. Present address: Institut für Festkörperphysik, Friedrich-Schiller-Universität Jena, Max-Wien-Platz 1, D-07743 Jena, Germany. Fax: 49 3641 947302.

Electronic address: wesch@pinet.uni-jena.de

[1] R. L. Fleischer, P. B. Price, and R. M. Walker, *Nuclear Tracks in Solids* (University of California Press, Berkeley, 1975).

[2] Proceedings of the Second International Symposium on Swift Heavy Ions in Matter, Bensheim/Darmstadt, 1992 [Radiat. Eff. Defects Solids **126** (1–4), (1993)]; Proceedings of the Third International Symposium on Swift Heavy Ions in Matter, Caen, 1995 [Nucl. Instrum. Methods Phys. Res. B **107/108** (1995)].

[3] A. Miotello and R. Kelly, Nucl. Instrum. Methods Phys. Res. B **122**, 458 (1997).

[4] S. Furuno, H. Otsu, K. Hojou, and K. Izui, Nucl. Instrum. Methods Phys Res. B **107**, 223 (1996).

[5] J. Vetter, R. Scholz, and N. Angert, Nucl. Instrum. Methods Phys. Res. B **91**, 129 (1994).

[6] A. M. Zaitsev, Nucl. Instrum. Methods Phys. Res. B **62**, 81 (1991).

[7] D. P. Erchak and V. G. Efimov, Nucl. Instrum. Methods Phys. Res. B **69**, 443 (1992).

[8] M. Levalois, P. Bogdanski, and M. Toulemonde, Nucl. Instrum. Methods Phys. Res. B **63**, 14 (1992).

[9] M. Levalois, I. Lhermitte-Sebire, P. Marie, E. Paumier, and J. Vicens, Nucl. Instrum. Methods Phys. Res. B **107**, 239 (1996).

[10] M. Mikou, R. Carin, P. Bogdanski, and R. Madelon, Nucl. Instrum. Methods Phys. Res. B **107**, 246 (1996).

[11] S. A. Karamyan, Nucl. Instrum. Methods Phys. Res. B **51**, 354 (1990).

[12] S. A. Karamyan, V. N. Bugrov, C. Ascheron, G. Otto, S. Yu. Platonov, and O. A. Yuminov, Radiat. Eff. Defects Solids **126**, 265 (1993).

[13] W. Wesch, E. Wendler, T. Bachmann, and O. Herre, Nucl. Instrum. Methods Phys. Res. B **96**, 290 (1995).

[14] L. Cliche, S. Roorda, M. Chicoine, and R. A. Masut, Phys. Rev. Lett. **75**, 2348 (1995).

[15] A. Gutzmann and S. Klaumünzer, Nucl. Instrum. Methods Phys. Res. B **127/128**, 12 (1997).

[16] K. Gärtner, Nucl. Instrum. Methods Phys. Res. B **132**, 147 (1997).

[17] J. P. Biersack and J. F. Ziegler, *The Stopping and Ranges of Ions in Matter* (Pergamon, New York, 1985), Vol. 1.

[18] E. Wendler, T. Opfermann, P. Müller, and W. Wesch, Nucl. In-

strum. Methods Phys. Res. B **106**, 303 (1995).
[19] E. Wendler, T. Opfermann, and P. I. Gaiduk, J. Appl. Phys. **82**, 5965 (1997).
[20] J. F. Gibbons, Proc. IEEE **60**, 1062 (1972).
[21] M. Toulemonde, G. Fuchs, N. Nguyen, F. Studer, and D. Grault, Phys. Rev. B **35**, 6560 (1987).
[22] A. Meftah, F. Brisard, J. M. Constantini, M. Hage-Ali, J. P. Stoquert, F. Studer, and M. Toulemonde, Phys. Rev. B **48**, 920 (1993).
[23] Z. G. Wang, Ch. Dufour, B. Cabeau, J. Dural, G. Fuchs, E. Paumier, F. Pawlak, and M. Toulemonde, Nucl. Instrum. Methods Phys. Res. B **107**, 175 (1996).
[24] M. Toulemonde, Ch. Dufour, and E. Paumier, Phys. Rev. B **46**, 14 362 (1992).
[25] Z. G. Wang, Ch. Dufour, E. Paumier, and M. Toulemonde, J. Phys.: Condens. Matter **6**, 6733 (1994).
[26] P. Stampfli and K. H. Bennemann, Appl. Phys. A: Mater. Sci. Process. **60**, 191 (1995).
[27] P. Stampfli and K. H. Bennemann, Phys. Rev. B **49**, 7299 (1994).
[28] W. Wesch, E. Wendler, G. Götz, K. Unger, H. Röppischer, Chr. Resagk, Phys. Status Solidi B **130**, 539 (1985).
[29] J. M. Poate, Nucl. Instrum. Methods Phys. Res. **209/210**, 211 (1983).